mm-Wave Dielectric Resonator Antenna (DRA) with Wide Bandwidth for the Future Wireless Networks

Ojaroudiparchin, Naser; Shen, Ming; Pedersen, Gert F.

Published in:
Microwave, Radar and Wireless Communications (MIKON), 2016 21st International Conference on

DOI (link to publication from Publisher):
10.1109/MIKON.2016.7492007

Publication date:
2016

Document Version
Early version, also known as pre-print

MM-Wave Dielectric Resonator Antenna (DRA) with Wide Bandwidth for the Future Wireless Networks

Naser Ojaroudiparchin, Ming Shen, and Gert Frølund Pedersen
Antennas, Propagation, and Radio Networking (APNet) Section
Department of Electronic Systems, Faculty of Engineering and Science
Aalborg University, DK-9220, Aalborg, Denmark
{naser, mish, gfp}@es.aau.dk

***Abstract*—This paper represents the design of a compact dielectric resonator antenna (DRA) for the future fifth generation (5G) applications. The antenna consists of a cylindrical-ring dielectric resonator (DR) mounted on a low-cost FR-4 surface, and a full ground plane. The antenna is fed by a coaxial probe with its inner conductor located adjacent to the DR. The antenna has good performance in terms of input-matching, gain and efficiency characteristics. The variation of the antenna properties in terms of gain and efficiency are less than 2 and -0.5 dB across its impedance pass-band (20 to 35 GHz for S_{11}<-10 dB). Using the proposed DRA design, the radiation characteristics of 2×2, 4×4, and 8×8 planar arrays are investigated. In addition, the fundamental properties of the 1×8 linear array have been discussed. Simulations have been done to validate the feasibility of the proposed DRA for the future 5G wireless networks.**

Keywords—coaxial-fed DRA; future communications; mm-Wave applications

I. Introduction

In the last decade, dielectric resonator antennas (DRAs) have received considerable amount of research efforts owning to their attractive features such as compact size, high radiation efficiency, wide bandwidth, easy excitation [1-3]. DRAs are available in various shapes and can be fed through multiple feeding mechanisms [4]. Due to these attractive advantages, they could be highly suitable for the development of the future wireless communications.

Compared with the current and previous generations (1G to 4G) of wireless communications, fifth generation (5G) networks are expected to use the millimeter (mm-Wave) frequency bands (beyond 10 GHz) due to the growing need for wider bandwidths and higher data rates [5-7]. Moving to the mm-Wave frequencies requires careful considerations in the design of antennas [8]. Our work represents an initial study on the design of DRAs for the future 5G applications.

A compact cylindrical-ring DR with dielectric constant of 10 has been used as a main radiator in the proposed design. The antenna is designed on a low-cost FR-4 substrate and fed by a coaxial probe. It is working in the frequency range of 20 to 35 GHz. The simulated results show that the proposed DRA exhibits good features in terms of different parameters. The configuration of the proposed DRA, its impedance bandwidth, and radiation properties have been presented and investigated in Section II. The performances of the linear and planar arrays with different number of DRA radiators (2×2, 4×4, and 8×8) have been described in Sections III and IV, respectively. Last Section concludes the presented study.

II. The Proposed DRA

Figure 1 displays the configuration of the proposed DRA fed by a coaxial probe. The inner conductor of the coaxial cable is located adjacent to the DR for signal transition. It can be also located within the DR. The length of the protruded inner conductor has a significant impact on the antenna performance. An FR-4 dielectric with 1 mm thickness and permittivity of 4.3 is used as the substrate. It has the same dimension as the ground plane, occupying an area of $W_S \times L_S$. The employed DR has a low permittivity (ε_{rd}) of 10 and a loss tangent (δ) of 0.0001 which is located at the center of the substrate. The low permittivity ($10 \le \varepsilon_{rd} \le 100$) of DR can help achieve wide bandwidth [9-10]. The parameter values of the designed antenna and its linear array are specified in Table 1.

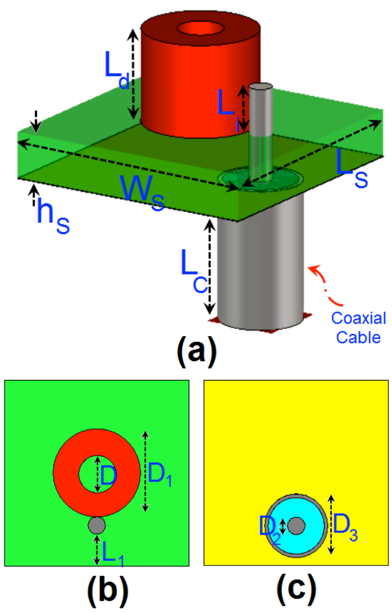

Fig. 1. The proposed coaxial-fed DRA, (a) 3D schematic, (b) front profile, and (c) back profile (Full-GND).

TABLE I. VALUES OF THE PROPOSED DRA PARAMETERS

Parameter	W_S=	L_S	h_S	W_a	L_a	L_d
Value (mm)	5.5	5.5	1	44	5.5	2
Parameter	L_C	L_i	D	D_1	D_2	D_3
Value (mm)	3	1	1	2.5	0.5	1.8

The simulated S_{11} characteristic of the antenna is depicted in Fig. 2. As shown, the impedance bandwidth of the proposed DRA for -10 dB is from 20 GHz to 35 GHz which is equivalent to a > 50% fractional bandwidth (FBW). However, the antenna bandwidth and its impedance-matching can be tuned by adjusting the values of the critical parameters such as the inner conductor length and the inner diameter of DR.

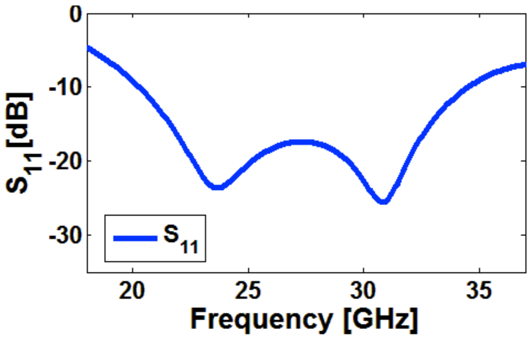

Fig. 2. S_{11} characteristic of the designed DRA.

The S_{11} curves of the antenna for various values of L_i (length of the inner conductor) and D (inner diameter of the cylindrical-ring) are illustrated in Fig. 3. As mentioned above, different values of the antenna critical parameters have main effects on the frequency response of the proposed antenna.

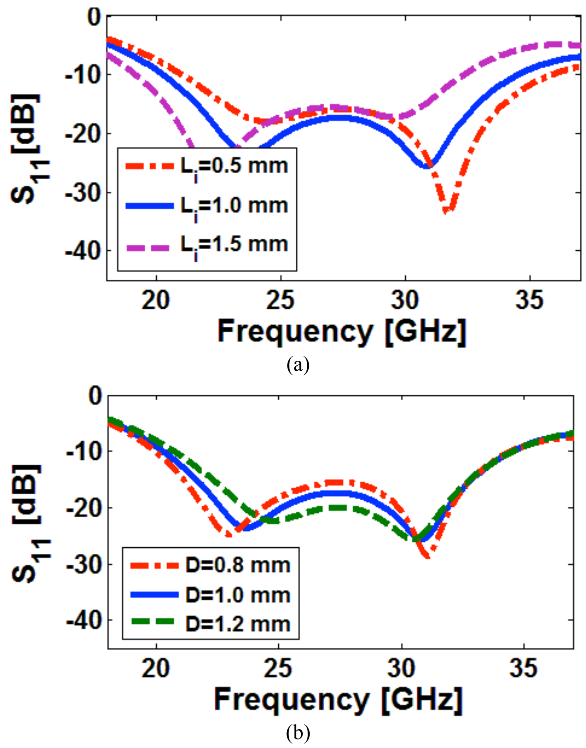

Fig. 3. Simulated S_{11} curves for different values of (a) L_i, and (b) D.

From this result, it can be observed that for L_i=1 mm & D=1 mm, the antenna has a good impedance matching at the desired frequency range of 20-35 GHz. According to the H-field distribution for the presented antenna at the center frequency of the antenna response (27 GHz) shown Fig. 4, the strong distribution arises around the inner conductor and the DR. Therefore, a significant impact of the inner conductor on the antenna performance can be found.

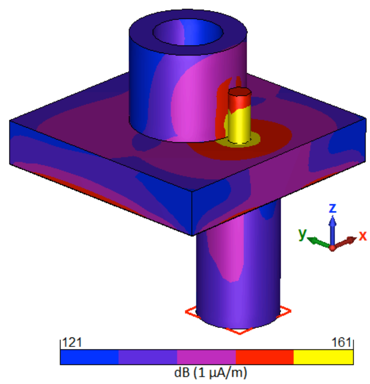

Fig. 4. Simulated H-field distribution of the DRA at 27.5 GHz.

Due to the wide bandwidth, the radiation patterns of the proposed antenna at lower, middle, and upper frequencies (23, 27, and 31 GHz, respectively) are studied and illustrated in Fig. 5. In addition, their 2D-ploar patterns have been represented in Fig. 6. Based on the simulations, similar performances with good realized gain values have been obtained for the proposed antenna.

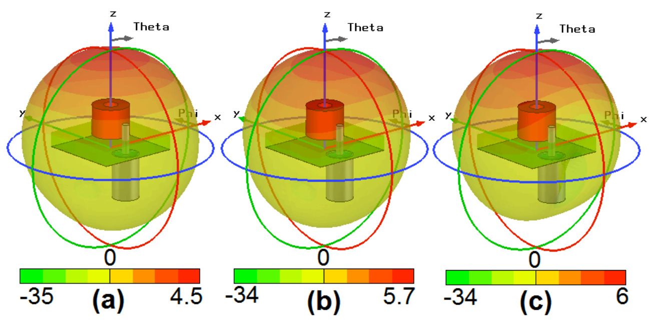

Fig. 5. 3D radiation patterns of the DRA at (a) 23 GHz, (b) 27 GHz, and (c) 31 GHz.

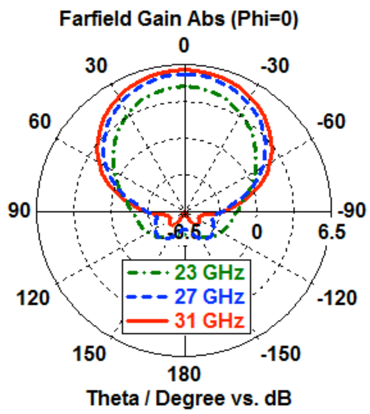

Fig. 6. 2D-ploar radiation patterns of the antenna at different frequencies.

Furthermore, as shown in Fig. 6, the antenna has low back-lobes at different frequencies in the operation band which indicates a consistent performance behavior versus frequency. In order to demonstrate that the antenna actually radiates over its operation band, its radiation properties in terms of maximum gain, radiation and total efficiencies are presented in Fig. 7. More than -0.5 efficiencies and 4 dBi maximum gain have been obtained in the operation frequency band. As shown, the antenna has good performance with low variations on the parameters values.

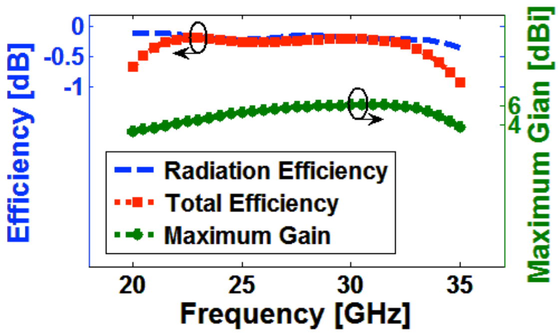

Fig. 7. Simulated fundamental radiation properties of the DRA over its operation frequency band.

III. 1×8 Linear Array of the Proposed DRA

The configuration of the DRA array is displayed in Fig. 8. It consists of eight element DRAs arranged in a linear form with interval of d=λ/2 (center frequency at 27 GHz).

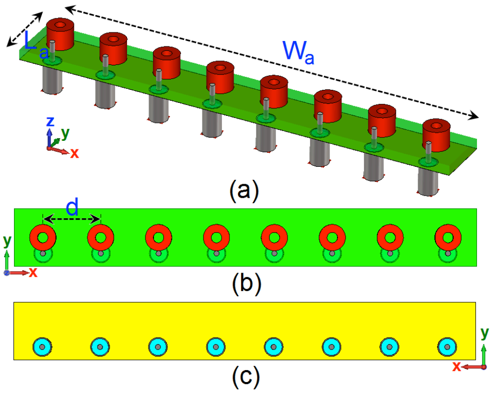

Fig. 8. (a) Side, (b) top, and (c) bottom views of the linear DRA array.

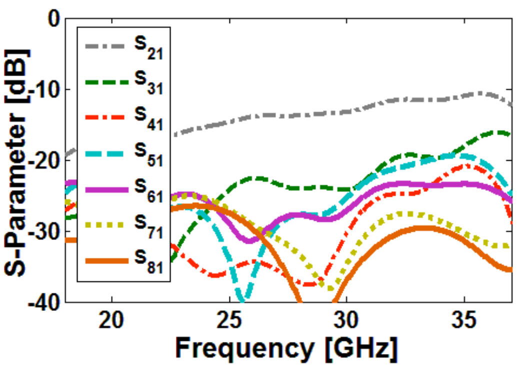

Fig. 9. The simulated S_{21} to S_{81} characteristics of the linear array.

Figure 9 shows the simulated S parameters of the array. As shown, the array has a good performance in the frequency range from 20 to 35 GHz with a mutual coupling (S_{21}) less than -14 dB between the radiators.

The radiation beams of the linear array with the directivity values at 0, 30, and 60 degrees are shown in Fig. 10. As can be observed, the designed array has good beam steering property with high-level directivities and low back-lobes. The simulated realized gains (IEEE gain × mismatch losses) of the linear DRA array at different angles are illustrated in Fig. 11. It can be seen that the array has good gain levels at different scanning angles.

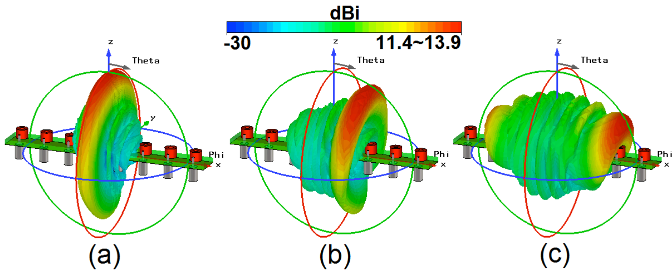

Fig. 10. The array radiation beams at, (a) 0°, (b) 30°, and (c) 60°.

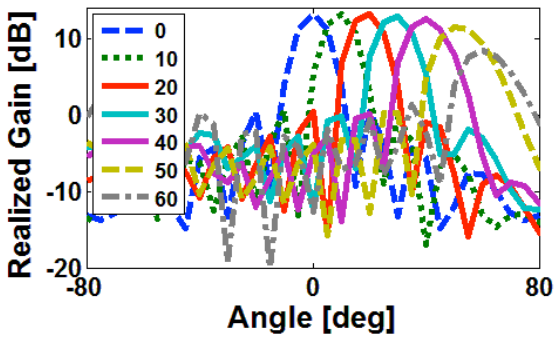

Fig. 11. Simulated realized gains of the linear array.

Simulated directivity and radiation efficiency characteristics of the array versus scanning angle are shown in Fig. 12. As can be seen, the radiation efficiency of the antenna is higher than -0.25 dB (95%). In addition, the antenna directivity is more than 11 dBi at the different scanning angles. It should be noted that due to the symmetric radiation patterns of the array elements, the performance for minus (-) angles are not shown.

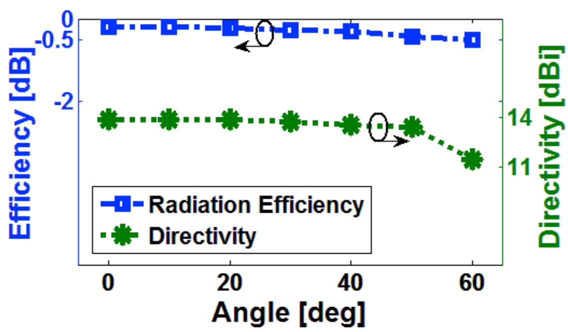

Fig. 12. The simulated directivity and efficiency properties of the DRA array versus scanning angle.

IV. Planar DRA Arrays

In this section, the radiation performances of the planar arrays with three different numbers of the DRAs have been investigated. Figure 13 shows the configurations of the DRA arrays in size of 2×2, 4×4, and 8×8.

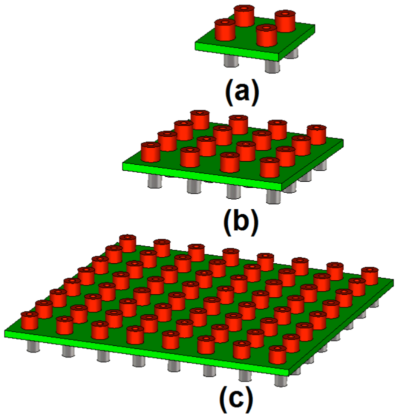

Fig. 13. The planar arrays, (a) 2×2, (b) 4×4, and (c) 8×8.

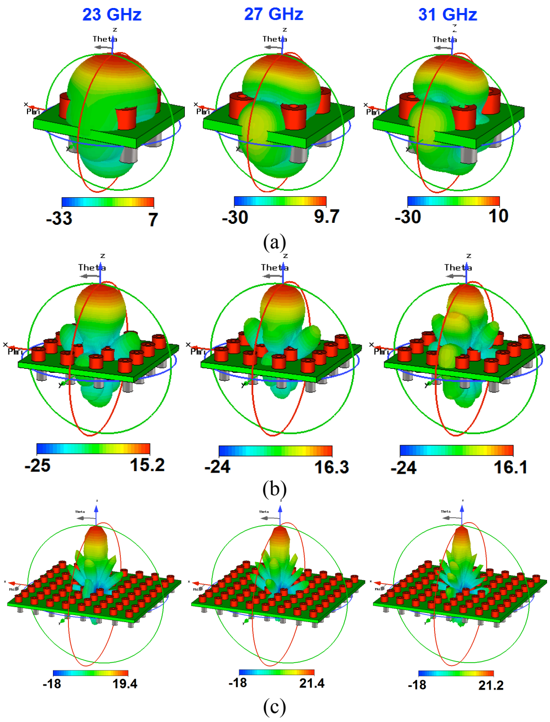

Fig. 14. 3D views of the radiation beams at 0° for (a) 2×2, (b) 4×4, and (c) 8×8 planar arrays.

Figure 14 illustrates the radiation beams of the planar DRA arrays when their beams are tilted to 0° elevation. It is clear that the planar arrays of the DRA have good radiation behaviors with high-level gains and directive patterns at different frequencies of the operation band. The investigated planar arrays also have high efficiency characteristics.

V. Conclusion

This paper presents a new compact design of the DRA with broad bandwidth for future 5G systems. The antenna is designed on a low-cost FR-4 substrate and fed by a coaxial probe. The operation frequency range of the antenna is from 20 GHz to 35 GHz. Furthermore, using the proposed design, the performances of DRA arrays with different number of radiation elements are investigated and good results have been obtained. Simulated results show that the proposed DRA is highly suitable for the development of the future wireless communications. In addition, the proposed arrays have a low profile with symmetric configurations and could be integrated with wireless devices.

References

[1] A. Petosa, A. Ittipiboon, Y. M. M. Antar, and D. Roscoe, "Recent advances in dielectric resonator antenna technology," *IEEE Antennas and Propagation Magazine*, vol. 40, pp. 35-48, 1998.

[2] X. L. Liang and T. A. Denidni, "H-shaped dielectric resonator antenna for wideband applications," *IEEE Antennas Wireless Propagation Letters*, vol. 7, pp. 163–166, 2008.

[3] G. Mehakand and S. K. Sharma, "Wide-bandwidth dielectric resonator antenna with omni-directional radiation patterns for beam focusing properties in a circular array," *International Journal of RF and Microwave Computer-Aided Engineering*, vol. 24, pp. 92–101, 2014.

[4] A. Petosa, "*Dielectric resonator antenna handbook,*" Artech House, Boston/London, 2007.

[5] J. Wells, "Faster than fiber: The future of multi-Gb/s wireless," *IEEE Microwave Magazine*, vol. 10, pp.104-112, 2009.

[6] Y. Wang, et *al.*, "5G mobile: Spectrum broadening to higher-frequency bands to support high data rates," *IEEE Vehicular Technology Magazine*, vol. 9, pp. 39-46, 2014.

[7] A. Osseiran, *et al.*, "Scenarios for 5G mobile and wireless communications: the vision of the METIS project," *IEEE Commun. Mag.,* vol. 52, pp. 26-35, 2014.

[8] S. Rajagopal, *et al.*, "Antenna array design for multi-Gbps mm-wave mobile broadband communication," in *IEEE Globecom*, Dec. 2011.

[9] A. Kishk, *et al.*, "Slot excitation of the dielectric disk radiator," *IEEE Transactions on Antennas and Propagations*, vol. 43, pp. 198–201, 1995.

[10] K. M. Luk and K. W. Leung, "*Dielectric resonator antenna*," Research Studies Press, Baldock, England, 2003.